Paper 169

Proceedings of the Eleventh International Conference
on Computational Structures Technology,
B.H.V. Topping, (Editor),
Civil-Comp Press, Stirlingshire, Scotland

Dynamic Instability of Circular Cylindrical Shells subject to Base Excitation

F. Pellicano
Dipartimento di Ingegneria Meccanica e Civile
Universita di Modena e Reggio Emilia, Italy

Abstract

This paper is focused on the experimental and theoretical analysis of circular cylindrical shells subject to base excitation. The shell axis is vertical, it is clamped at the base and connected to a rigid body on the top; the base provides a vertical seismic-like excitation. The goal is to investigate the shell response when a resonant harmonic forcing is applied: the first axisymmetric mode is excited around the resonance at relatively low frequency and low amplitude of excitation. A violent resonant phenomenon is experimentally observed as well as an interesting saturation phenomenon close to the previously mentioned resonance. A theoretical model is developed to reproduce the experimental evidence and provide an explanation of the complex dynamics observed experimentally; the model takes into account geometric shell nonlinearities, electro-dynamic shaker equations and the shell shaker interaction.

Keywords: shells, nonlinear dynamics.

1 Introduction

Several commercial software allow to carry out static, stability and vibration analyses; however, regarding the shell dynamics, such kind of analyses are generally reliable in the linear filed, i.e. very small deformations. Problems like global stability, post-critical behaviours and nonlinear vibrations cannot yet be accurately analysed with commercial software; on such fields there is need of further development of computational models.

Readers interested to deepen the literature are suggested to read Refs.[1-6]: some topics of extreme importance need further investigations: dynamic stability, post-critical behaviour, sensitivity to imperfections, nonlinear vibrations and fluid structure interaction.

Kubenko and Koval'chuk [7] published an interesting review on nonlinear problems of shells, where several results were reported about parametric vibrations; in such review the limitations of reduced order models were pointed out.

In Ref. [8] a new method, based on the nonlinear Sanders Koiter theory, suitable for handling complex boundary conditions of circular cylindrical shells and large amplitude of vibrations. The method was based on a mixed expansions considering orthogonal polynomials and harmonic functions. Among the others, the method showed good accuracy also in the case of a shell connected with a rigid body; this method is the starting point for the model developed in the present research.

Mallon et. al [9] studied circular cylindrical shells made of orthotropic material, the Donnell's nonlinear shallow shell theory was used with a multimode expansion for discretization (PDE to ODE). The theoretical model considered also the shaker-shell interaction; such work is strictly related to the present paper for which concern theory and experiments; here a further step toward improved modelling and complete understanding of complex dynamic phenomena is attempted, in addition here experiments show great coherence with theoretical results.

In the present paper, experiments are carried out on a circular cylindrical shell, made of a polymeric material (P.E.T.) and clamped at the base by gluing its bottom to a rigid support. The axis of the cylinder is vertical and a rigid disk is connected to the shell top end.

Nonlinear phenomena are investigated by exciting the shell using a shaking table and a sine excitation. Shaking the shell from the bottom induces a vertical motion of the top disk that causes axial loads due to inertia forces. Such axial loads generally give rise to axial-symmetric deformations; however, in some conditions it is observed experimentally that a violent resonant phenomenon takes place, with a strong energy transfer from low to high frequencies and huge amplitude of vibration. Moreover, an interesting saturation phenomenon is observed: the response of the top disk was completely flat as the excitation frequency was changed around the first axisymmetric mode resonance.

A semi-analytical approach is proposed for reproducing experimental results and giving a deeper interpretation of the observed phenomena. The shell is modelled using the nonlinear Sanders Koiter shell theory; in modelling the system the effect of the top disk was accounted for applying suitable boundary conditions and considering its inertial contribution; moreover, the interaction between the shell-disk and the electro-dynamic shaking table was included in the modelling. The shell displacement fields are represented by means of a mixed series (harmonic functions and orthogonal polynomials), which are able to respect exactly geometric boundary conditions; an energy approach, based on the Lagrangian equations, is used to obtain a set of ODE that represents the original system with good accuracy.

Comparisons between experiments and numerical results show a good behaviour of the model, numerical analyses furnish useful explanations about the instability phenomena that are observed experimentally.

2 Experimental setup and results

In the present section the problem under investigation is described by means of experimental results. The description follows the history of the present research, which started from experimental observations that led the author in developing the theoretical model.

2.1 The setup

The system under investigation is described in Figures 1 and 2; a circular cylindrical shell, made of a polymeric material (P.E.T.), is clamped at the base by gluing its bottom to a rigid support ("fixture"); the connection is on the lateral surface of the shell, in order to increase the gluing surface, see Figure 1; on the top, the shell is connected to a disk made of aluminium alloy, such disk is not externally constrained; therefore, it induces a rigid body motion to the top shell end.
The system data are the following: $\rho = 1366\,\frac{\text{kg}}{\text{m}^3}$, $\nu = 0.4$, $E = 46\times 10^8\,\text{N/m}^2$; mass of the top disk 0.82kg. The geometry is: radius R=43.88 10^{-3}m, length L=96 10^{-3}m thickness h=0.25 10^{-3}m.

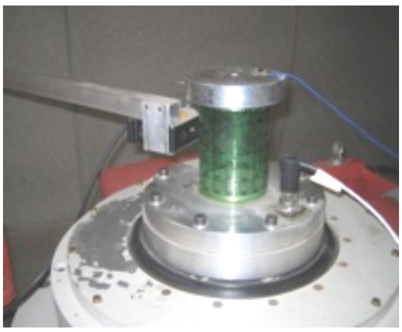

Figure 1. Experimental setup

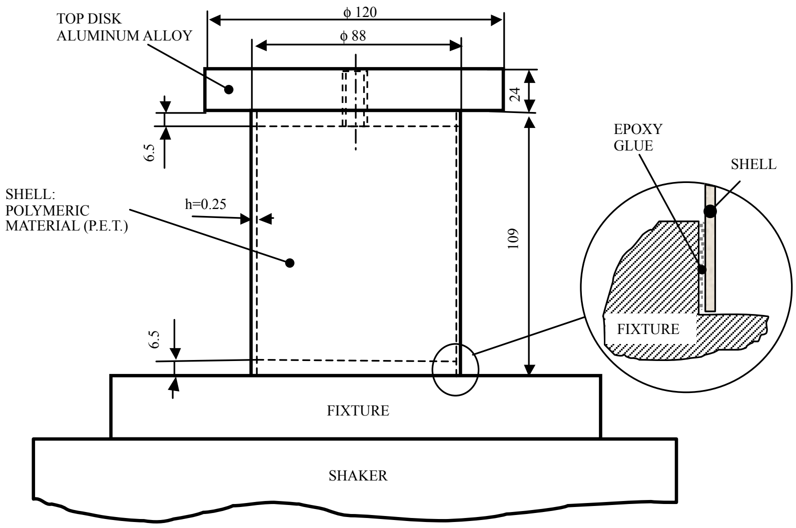

Figure 2. System geometry

The fixture is bolted to a high power shaker (LDS V806, 13000N peak force, 100g, 1-3000Hz band frequency).
When the base of the shell is excited by the shaker, a fluctuating vertical move is determined, such base movement results in a seismic-like excitation for the shell; the rigid body motion generates big inertia forces on the top disk that cause an axial shell loading. In particular, the vertical excitation can cause the resonance of the first axisymmetric mode of the shell, Figure 3; therefore, the base excitation can be amplified inducing large axial stresses on the shell.

2.2 Experimental results

Initially, an experimental modal analysis is carried out (about 80 points are considered) in order to extract (identify) natural frequencies, modal damping and mode shapes from experimental data.
The natural frequencies of the system are reported in Table 1, the corresponding mode shapes are represented in Figure 3.

Mode		Natural frequencies [Hz]				
		Experimental frequency	Theory		Finite elements	
k	*n*		Frequency	Error %	Frequency	Error%
first beam like mode *n*=1		95	96	1.1	93	2.1
1	0	314	322	2.5	314	0
second beam like mode *n*=1		438	432	2.5	424	3.2
1	6	791	797	0.8	782	1.1
1	7	816	802	1.7	802	1.7
1	5	890	888	0.2	885	0.6
1	8	950	926	2.5	918	3.4
1	9	1069	1016	5.0	1103	3.2

Table 1. Natural frequencies and mode shape description [8].

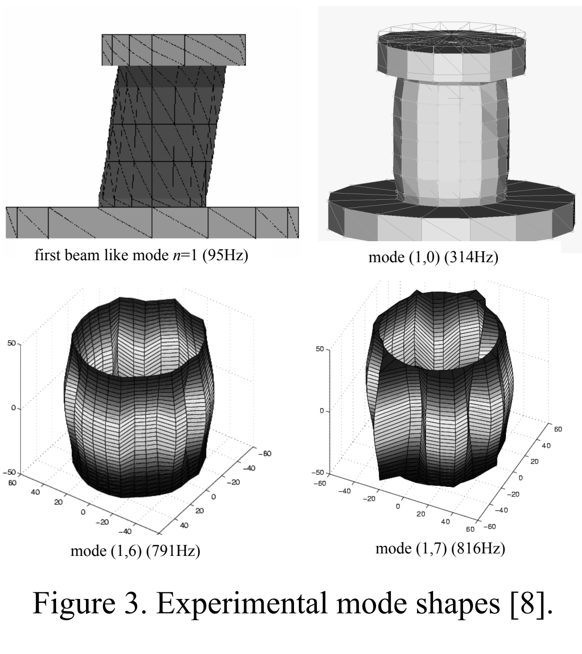

Figure 3. Experimental mode shapes [8].

The first three modes of Table 1 present a shape that includes the top disk motion; the second mode (first axisymmetric mode) shows a simple translational motion of the top disk, see Figure 3; shell like modes (modes after the third of Table 1) behave like clamped-clamped shell modes, i.e. the top disk does not move. For the linear theory, shell like modes of a perfect shell are not directly excited by a translational base motion on the shell axis, because the top disk motion cannot pump energy in such modes. The only prediction that could be done using linear models is to consider the time varying axial forces caused by the top mass acceleration, this will lead to a time varying linear system, which could undergo to parametric instabilities of Mathieu type; therefore, linear theories could be able to analyze the instability boundaries only.

Experiments proved that, when the shell is excited harmonically from the base, with an excitation frequency close to the first axisymmetric mode, complex dynamic scenarios appear and the energy pumped in the system at low frequency spreads over a wide range of the spectrum.

Tests are carried out using a seismic sine excitation, close to the resonance of the first axisymmetric mode (m=1, n=0).

The complexity and violence of vibrations due to nonlinear phenomena gave several problems to closed loop controllers of the shaking table; therefore, an open loop approach was chosen.

The accelerations of the base, the top, and the displacement of the shell lateral surface are measured.

Figures 4a-e represent the amplitudes of vibration in terms of acceleration (base and top disk vibration) or displacement (measured on the lateral surface of the shell, the vertical position is on the middle): during experiments the input voltage was sinusoidal ($v(t)=v_0\sin(2\pi f t)$, v_0=0.07V) and the frequency was moved step by step (stepped sine approach with a frequency step of 0.3Hz) starting from high frequency, 340Hz, and reducing up to 290Hz; the sampling frequency was about 6400Hz.

Figure 4a shows that the maximum excitation (base motion) is between 8 and 14 g; there is a strong interaction between the shaker and the shell-disk.

The top disk vibration (Figure b) increases as the first axisymmetric mode resonance is approached, from 340 to 333Hz the top disk response follows the usual behaviour expected by a linear resonance. The top disk vibration amplitude remains flat from 322 to 295 Hz.

For frequencies higher than 333Hz the shell vibration is small, about 0.04 mm (about 16% with respect to the shell thickness, 0.25mm), Figure 4c; reducing the excitation frequency below 333Hz, the shell vibration amplitude suddenly grows up, at 331.5 Hz the amplitude is 0.57 mm, the increment is 1325%; such huge increment takes place in a narrow frequency band, i.e. from 333 Hz to 331.4 Hz (about 0.5% frequency variation). Another jump in the shell response is observed from 325 Hz (0.75 mm amplitude) to 320 Hz (1.53 mm), i.e. 104% increment in terms of amplitude in 5 Hz. The response remains almost flat from 300 to 296Hz, the amplitude oscillates around 1.5 mm; then at 295 Hz the phenomenon suddenly disappears (0.022mm amplitude).

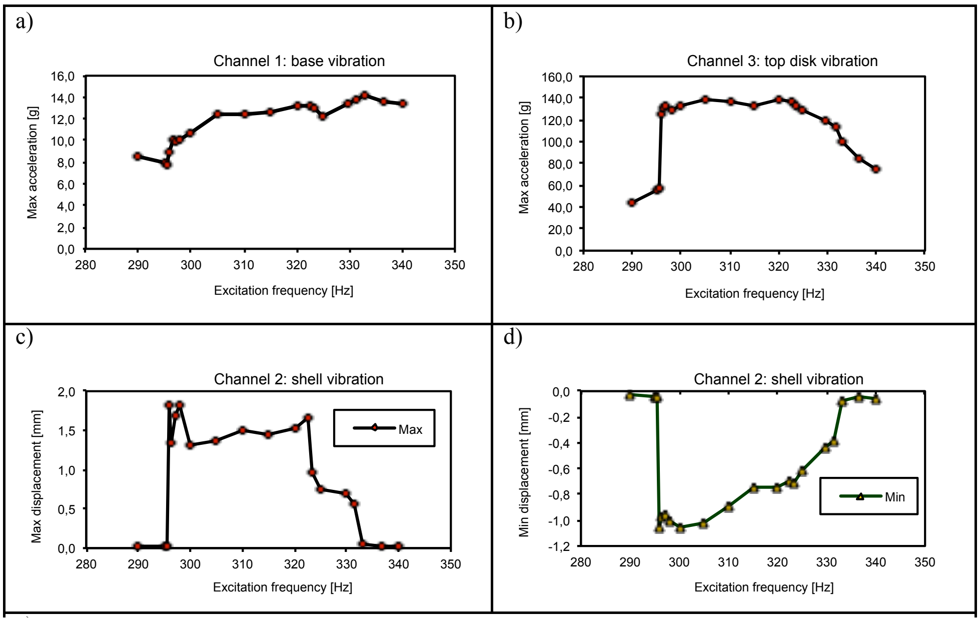

Figure 4. Experimental results, amplitude, harmonic excitation: a) base excitation amplitude (acceleration [g]), b) top disk amplitude (acceleration [g]), c) response on the shell mid-span (displacement [mm], positive inward), d) minimum response of the shell mid-span (displacement [mm], negative outward).

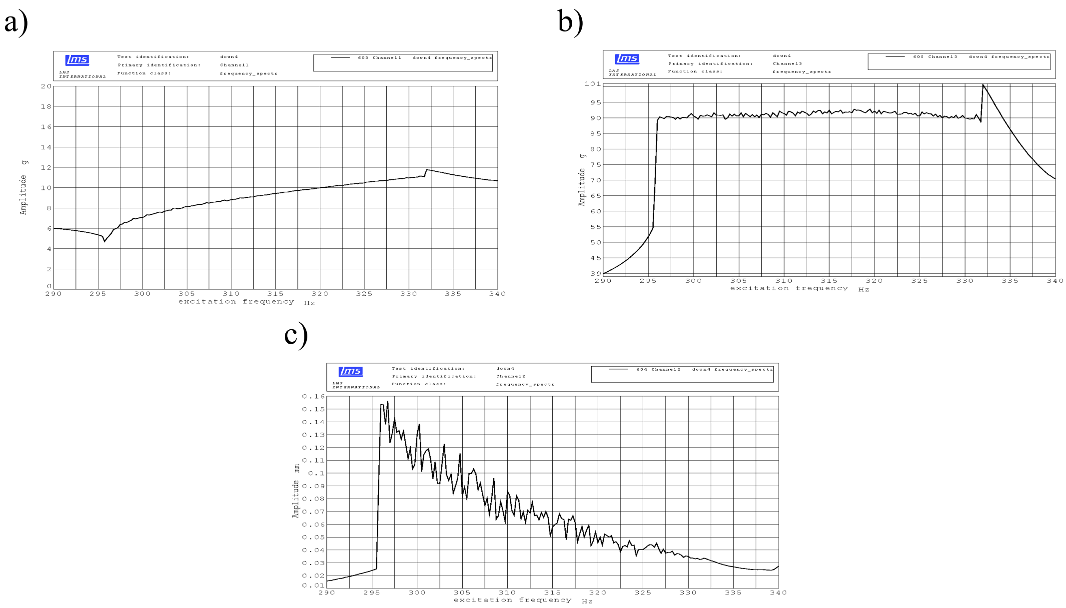

Figure 5. Experimental results, RMS, harmonic excitation: a) base excitation (acceleration [grms]), b) top disk (acceleration [grms]), c) response on the shell mid-span (displacement [mm] rms).

In Figure 5a-c this scenario is represented in terms of RMS, which is of interest as it represents the vibration energy of the phenomenon. Comments to Figures4a-e apply also to Figures 5a-c; however, considering the RMS one can clearly observe the saturation phenomenon (Figure 5b), the response of the top disk, in proximity of the resonance, becomes completely flat even though the excitation varies (remember that the excitation is open-loop). In terms of RMS, the shell vibration presents a jump at 296Hz, but the jump at 333Hz disappears; apparently, this is incoherent with Figure 4c, such incoherence is explained by checking the time response, which is characterized by a non-stationary behaviour and the presence of several spikes. Spikes have a direct influence the maximum of a signal, but the effect on the signal energy can be almost insensible, therefore it is not surprising a difference on representation of the dynamic scenario in terms of amplitude or RMS.

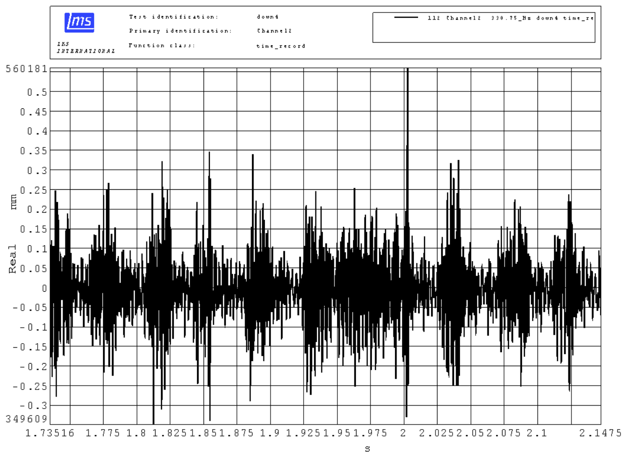

Figure 6. Lateral shell vibration (displacement mm), sine excitation, frequency 331Hz.

It is to note that the dynamic phenomenon is extremely violent, it is accompanied by a strong noise (hear protections are needed), the acceleration generated on the shell are surprisingly huge. For example if the amplitude is 3 mm, and we suppose the vibration is purely harmonic at 300 Hz, an approximate estimation of the acceleration is about 1100 g! Such estimate does not consider that the shell response is no more sinusoidal (see e.g. Figure 6), conversely it is non stationary and broad band, this means that the response spectrum contains high frequency components that can lead to a further increment of the acceleration. Some initial experiments carried out using accelerometers for the lateral shell vibration measurement, have shown accelerations up to 2000g!
Figure 7 shows the bifurcation diagram of Poincaré maps, this kind of representation is important to evaluate the stationarity of the response. In Figure 7 one can see that, outside the instability region (where violent vibrations are manifested), all measurement are close each other (one point), inside the instability region there is a spreading over a wide range (several points); this proves that the phenomenon is non stationary.

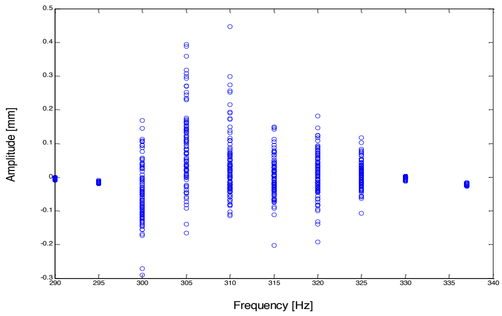

Figure 7. Bifurcation diagram. Experimental results.

The previous analysis furnishes a clear scenario about the dynamics of the system; however, it is referred to a particular excitation (sine input voltage amplitude 0.07V). In order to investigate the behaviour of the system as the excitation amplitude varies, several tests are carried out starting from 0.03 V. For each excitation level two tests are carried out increasing ("upward") and decreasing ("backward") the excitation frequency on the range 240-350 Hz; for each test the frequency boundaries of the instability are acoustically detected, i.e. by checking the change in the noise generated by the system. Results are presented in Figure 8, lines are the boundaries that separate the low vibration to high vibration regimes; the right boundary remains unchanged for downward and upward experiments, the left boundary is moved to the left in the case of backward tests; this means that the region were huge vibrations take place is wider when the excitation changes from high to low frequencies; this is typical of softening type nonlinearities.

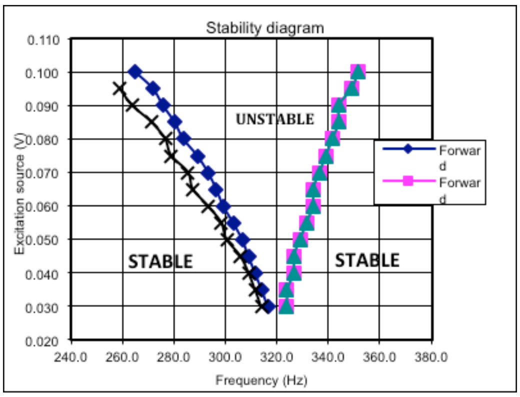

Figure 8. Stability region.

Figure 8 shows that the boundaries are almost straight lines starting from 320 Hz, they behave similarly to the classical Ince-Strutt diagrams referred to the instability regions of the Mathieu equation, which is the paradigm for problems with time varying coefficients (parametric excitation). For such reason, the region where huge vibrations take place is named here "instability region". Figure 8 suggests that the present phenomenon can be correlated to large in-plane loads, which are generated on the shell when the first axisymmetric mode undergoes to the resonance; such loads induce a parametric excitation on the shell like modes, which are high

frequency modes, this is an explanation of the energy transfer from low to high frequency.
The left and right boundaries of Figure 8 should theoretically touch each other at the bottom, depending on the damping; however, it was impossible to find experimentally such minimum, even if specific tests were attempted.
An energy transfer from low to high frequencies is quantified in Figures 9a,b; the spectrum of the Laser signal is represented. In the case of Figure 9a we are outside the unstable region and signal is dominated by the harmonic component referred to the excitation frequency (334 Hz), the other harmonic components are negligible as they are more than one order less than the dominant one (decade in log scale). Figure 9b shows that, when experiments are carried out inside the unstable region (316 Hz), the shell response presents a spectrum where the energy spreads over a wide range: from 316 to 1500 Hz one can see non-negligible harmonics; moreover, three dominant harmonics are present at about 316, 630 and 950 Hz (the discrete spectrum resolution does not allow great accuracy), i.e. the excitation frequency and its first two multiples.

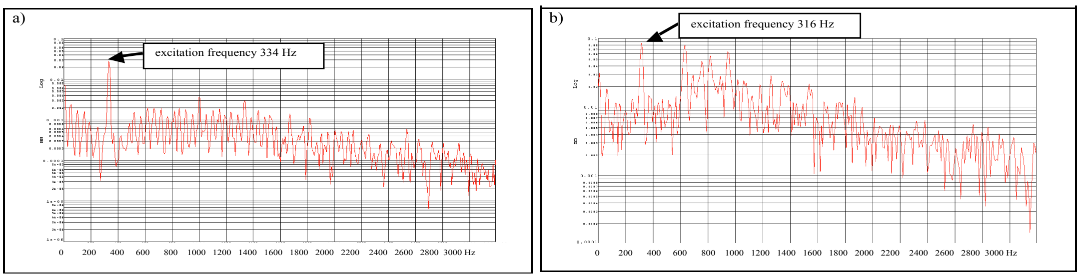

Figure 9. Lateral shell vibration, excitation 0.07V, spectra. a) 334Hz low vibration; b) 316Hz high amplitude vibration

The experiments show clearly the complexity of the problem under investigation, which can be summarized with the following three points:

1. There is a strong interaction among the excitation source (shaker) and the system under investigation (shell and top disk), this is proven by observing the behaviour of the base vibration compared with the top disk and shell vibration.
2. The violent dynamic phenomenon, observed around the resonance of the first axisymmetric mode, is due to a dynamic instability; this is proved by the stability diagram of Figure 9.
3. There is a nonlinear modal interaction among the directly excited mode (the first axisymmetric mode) and high frequency modes (shell-like modes), this is proved by observing that the top disk vibration amplitude have a flat region when the instability takes place, i.e. the energy flows from modes involving a disk motion to shell-like modes (no disk motion).

Such considerations are the starting point for developing a suitable theory able to reproduce the experimental observations and give a deeper understanding of the phenomenon.
A theory for the shell dynamics should include: nonlinear effects, top disk modelling including suitable boundary conditions and in-plane loads effect; a shaker-shell interaction model.

3 Modelling

The theoretical model of the shaker will be described as well as the theoretical shell modelling based on the nonlinear Sanders-Koiter theory.
The shaker used in the present experiments is an electromechanic machine, the main body is suspended on the ground by means of very soft gas suspensions (see Figure 10), which have the task of reducing forces transmitted to the ground. The power supply is given by an amplifier that is not represented in Figure 10, the amplifier furnishes the current both to the field coil and the armature coil; the amplifier input $E_0(t)$ is a low power and voltage signal (up to 1V), it is generated by an external device. The governing equations for the shaker are [9-10]:

$$L\dot{I}(t) + \Re I(t) + k_c \dot{U}_b(t) = E(t) \tag{1a}$$

$$m_0 \ddot{U}_b(t) + c_b \dot{U}_b(t) + k_b U_b(t) = k_c I(t) + F_{system}(t) \tag{1b}$$

where $\Re$ and L are the armature coil resistance and inductance respectively, and $E(t) = P_{amp}\left(b_{amp}\dot{E}_0(t) + E_0(t)\right)$

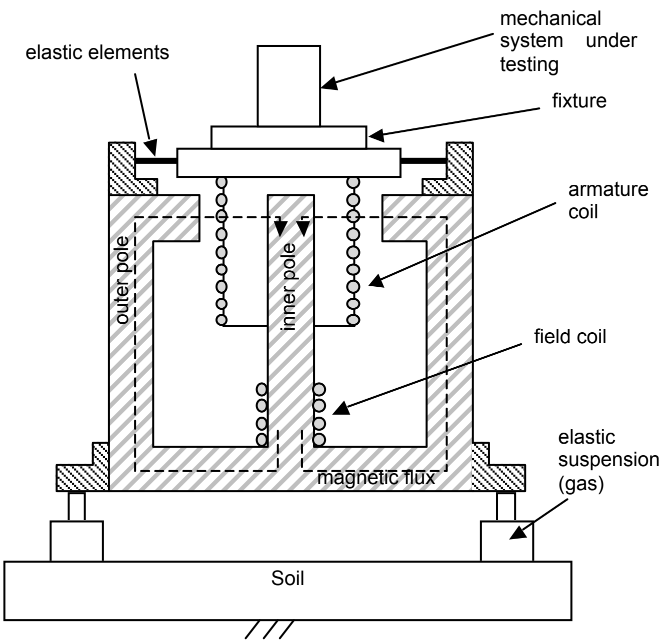

Figure 10. Electrodynamic shaker.

The geometry of a circular cylindrical shell is represented in Figure 11a; three displacement fields are represented: longitudinal u, circumferential v, radial w; the geometry of the shell is summarized by the following parameters: radius R, length L, thickness h.

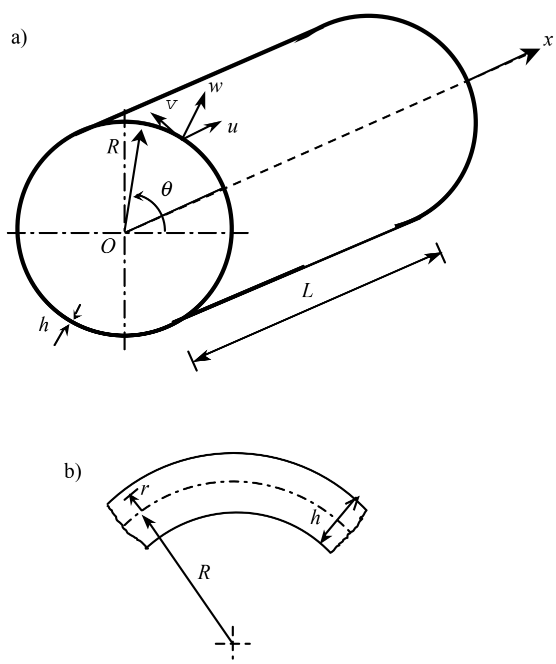

Figure 11. Shell model.

In the present work the nonlinear Sanders-Koiter theory is considered, this is a theory based on the Love's first approximation
Strain components ε_x, ε_θ and $\gamma_{x\theta}$ at an arbitrary point of the shell are:

$$\varepsilon_x = \varepsilon_{x,0} + r\,k_x \quad \varepsilon_\theta = \varepsilon_{\theta,0} + r\,k_\theta \quad \gamma_{x\theta} = \gamma_{x\theta,0} + r\,k_{x\theta} \tag{2}$$

where: $\varepsilon_{x,0}$, $\varepsilon_{\theta,0}$ and $\gamma_{x\theta,0}$ are the middle surface strains; k_x, k_θ and $k_{x\theta}$ are the curvature and torsion changes of the middle surface.
The elastic strain energy U_S of a circular cylindrical shell, neglecting the radial stress σ_r (Love's first approximation), is given by

$$U_S = \frac{1}{2} LR \int_0^{2\pi} \int_0^{1} \int_{-h/2}^{h/2} (\sigma_x \varepsilon_x + \sigma_\theta \varepsilon_\theta + \tau_{x\theta} \gamma_{x\theta}) \mathrm{d}\eta\, (1 + r/R) \mathrm{d}\theta \mathrm{d}r \tag{3}$$

where: $\sigma_x = \frac{E}{1-\nu^2}(\varepsilon_x + \nu \varepsilon_\theta)$, $\sigma_\theta = \frac{E}{1-\nu^2}(\varepsilon_\theta + \nu \varepsilon_x)$, $\tau_{x\theta} = \frac{E}{2(1+\nu)}\gamma_{x\theta}$, E is the Young's modulus and ν is the Poisson's ratio, the potential energy contains quadratic and higher order terms: the first one will lead to linear terms in the equations of motion and higher order terms will lead to nonlinear terms; $U_S = U_{S,linear} + U_{S,nonlinear}$, the kinetic energy T_S is given by

$$T_S = \frac{1}{2} \rho_S\, h\, L\, R \int_0^{2\pi} \int_0^{1} \left(\dot{u}^2 + \dot{v}^2 + \dot{w}^2 \right) \mathrm{d}\eta\, \mathrm{d}\theta, \tag{4}$$

where ρ_S is the mass density of the shell, the overdot denotes a time derivative.
External forces are considered by means of the virtual work
In order to carry out a linear vibration analysis $U_{S,LINEAR}$ is considered, see equation (7).
Following the approach developed in Ref.[8], modes of vibration are formally written as follows:

$$u(\eta,\theta,t) = U(\eta,\theta) f(t) \quad v(\eta,\theta,t) = V(\eta,\theta) f(t) \quad w(\eta,\theta,t) = W(\eta,\theta)\, f(t) \tag{10}$$

where: $U(\eta,\theta)$, $V(\eta,\theta)$ and $W(\eta,\theta)$ represent the modal shape, such shapes are described by means of a double series expansion, e.g: . $U(\eta,\theta)=\sum_{m=0}^{M_U}\sum_{n=0}^{N}\tilde{U}_{m,n}T_m^*(\eta)\cos n\theta$ where $T_m^*(\eta)=T_m(2\eta-1)$ and $T_m(\cdot)$ is the m-th order Chebyshev polynomial. The expansion allows to respect exactly the geometric boundary conditions.
Once the linear analysis is carried out the displacement fields are re-expanded using the eigenfunctions of the system, e.g. $u(x,\theta,t)=\sum_{j=1}^{N_{max}}U^{(j)}(x,\theta)f_{u,j}(t)$.
The shell shaker interaction and the effect of the top disk are taken into account in the energy approach based on the Lagrange equations. Details are omitted for the sake of brevity.

4 Numerical Analysis

Numerical analyses are carried out after a deep convergence analysis, details are omitted for the sake of brevity.

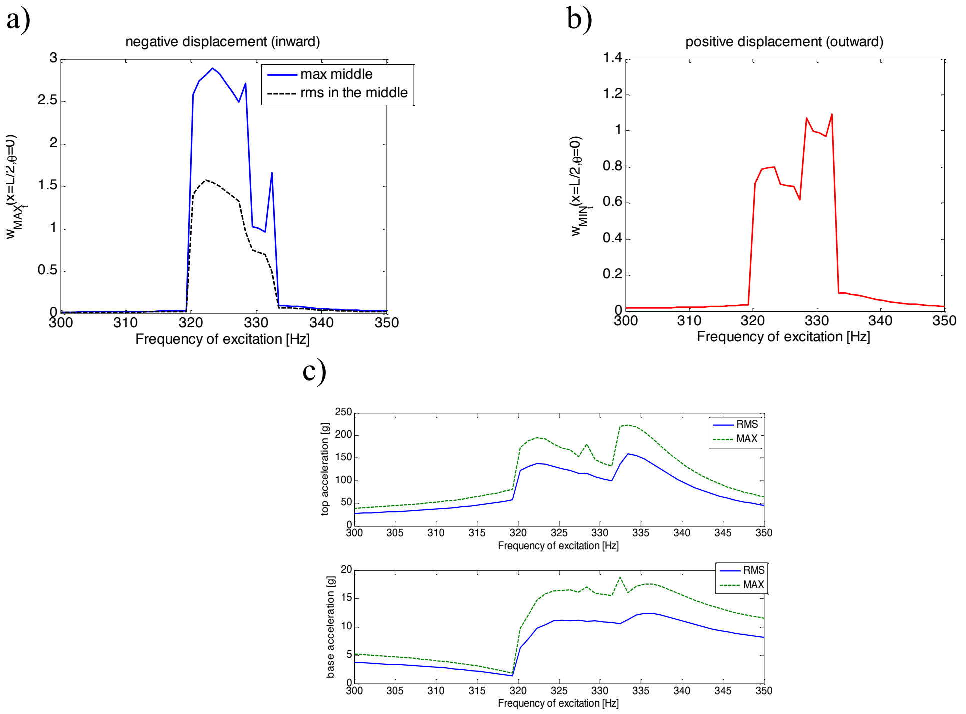

Figure 12. Amplitude frequency diagrams, numerical simulations, backward frequency sweep, shell vibration (mm). a) inward displacement and RMS(w); b) outward (positive) displacement. Position of the simulated point measurement: $x=\frac{L}{2}, \theta=0$, c) Top and base acceleration [grms]. Excitation source: 0.09V.

Results presented in Figure 12 are referred to a simulation carried out considering a sine excitation of the shaker with input voltage equal to 0.09V, this value is larger than the excitation used during the experiments (0.07V); however, below such value the numerical model did not detect any dynamic instability. Simulations are carried out by decreasing the excitation frequency. The issue about the voltage level is not really significant; indeed, the need of a voltage slightly larger than experiments is probably due to an underestimation of the amplifier gain: this quantity could be influenced by the operating conditions of the amplifier-shaker system. The simulation is carried out in the frequency interval 300-350Hz, decreasing the frequency; the onset of instability is found at 333.4Hz, below such frequency the vibration amplitude is magnified, at 329,4Hz a second increment of the vibration amplitude is detected leading the maximum inward deflection to 2.7mm, a further reduction of the frequency does not cause a big amplitude variation up to 319.3Hz, where the vibration level drops down to small amplitudes. The behavior is coherent with the experimental results, the numerical model overestimates the amplitude of vibration (experiments give 1.8mm max inward vibration) and underestimates the frequency range for which the instability appears (experimental instability range 295-333 Hz); this can be explained by the absence of companion modes and imperfections.

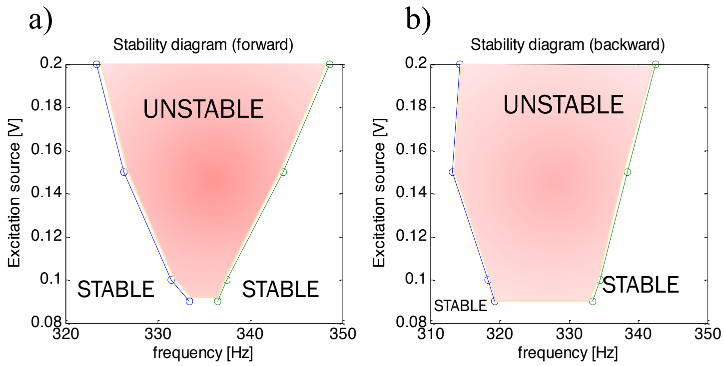

Figure 13. Stability boundaries.

Figure 13 shows the stability boundaries obtained numerically by varying both the excitation source voltage and frequency; the boundaries are coherent with experiments and similar to the Ince-Strutt diagrams referred to the Mathieu equation, this is a further confirmation that the instability is due to a parametric resonance. The boundaries, obtained by increasing the excitation frequency (forward), are quite similar to the experimental boundaries; numerical boundaries are moved up with respect to the experiments, i.e. for the same excitation voltage the experimental instability region is wider. Backward boundaries present a wider instability region for low voltage; moreover, left and right curves do not match at the bottom, this indicates that the boundaries search could be improved by using a more sophisticated search, which is however beyond the purposes of the present work.
Let us now consider an improved numerical model where companion modes are included in the expansion. It is worthwhile to point out the structures having symmetries are always characterized by double modes (also called *conjugate modes*) having the same frequency. In Figure 14 the representation of two conjugate modes is presented, the cross section of the shell is represented; indeed, the axial symmetry implies that the difference in shape of two conjugated modes appears only in the

circumferential direction. Shell conjugate modes have the same shape, but they are shifted of a quarter of wavelength in the circumferential direction. Obviously, axisymmetric modes do not have companions.

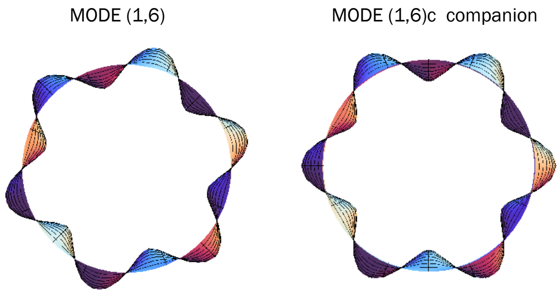

Figure 14. Conjugate modes: a shell-like mode and its companion.

If one includes companion modes in the displacement expansions (e.g. $u(x,\theta,t)=\sum_{j=1}^{N_{\max}}\left[U^{(j)}(x,\theta)f_{u,j}(t)+U_c^{(j)}(x,\theta)f_{u,j,c}(t)\right]$) the results of the simulations improve, see Figure 15. The instability phenomenon is captured better, i.e. the instability region is enlarged with respect to the case without companion mode participation (322-340Hz), the saturation is more evident and the amplitudes are closer to the experiments.

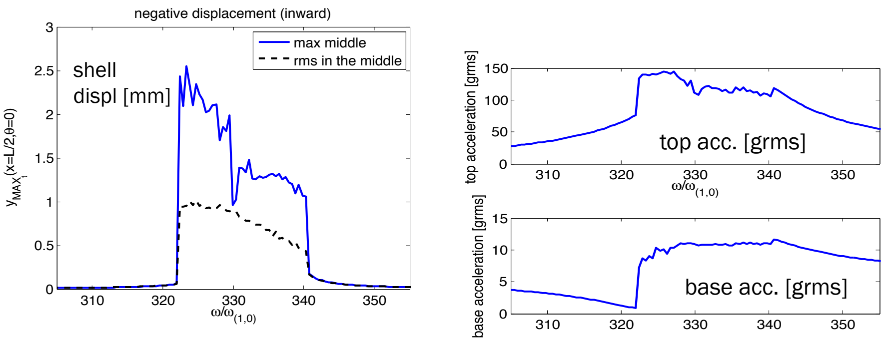

Figure 15. Companion mode participation. Amplitude frequency diagrams, numerical simulations, backward frequency sweep, shell vibration (mm). a) inward displacement and RMS(w); b) outward (positive) displacement. Position of the simulated point measurement: $x=\frac{L}{2}, \theta=0$. Excitation source: 0.09V.

The numerical model allows to deepen the comprehension of the instability mechanisms. Figure 16 shows that when the instability takes place, the mode (1,6) and its companion are activated; such modes are not directly excited by the axial forces generated by the seismic excitation, there is an auto-parametric excitation of the asymmetric modes (modes (m,n) with $n \neq 0$) due to the vibration of the resonant axisymmetric mode; the latter one is directly excited by the axial load produced by the inertia force of the top mass.

The energy transfer mechanism can be summarized as follows: outside the instability region the most important mode is the first axisymmetric one; inside the instability region mode (1,0) is driven by the resonant mode (1,6). When the instability takes place, the mode (1,6) is excited and absorb the most of the vibration energy, the energy inlet is provided at low frequency (close to the resonance of mode (1,0)), there is an energy transfer to the high frequency mode (1,6) a second modal activation is observed: mode (1,6c).

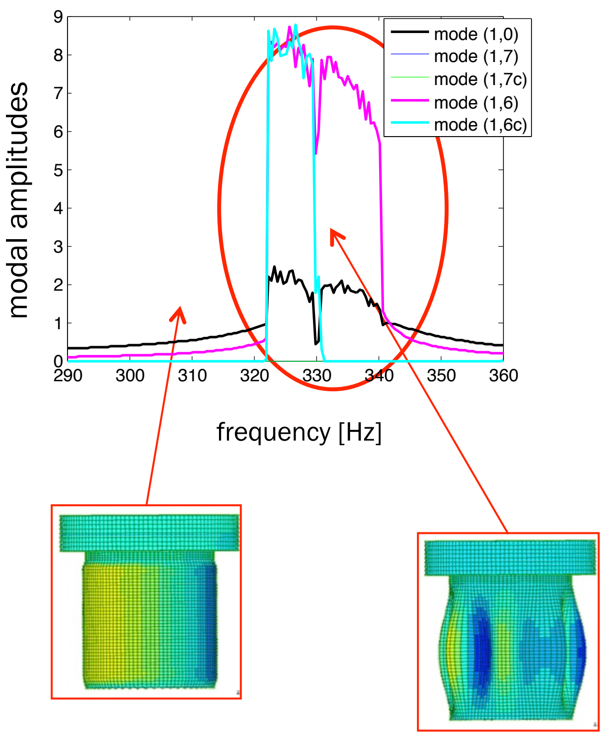

Figure 16. Amplitude frequency diagrams, numerical simulations, backward frequency sweep, modal amplitudes. Excitation source: 0.09V.

The analysis of the time histories is interesting: outside the instability region the response is regular and stationary (Figures 17 and 18), the spectrum presents peaks at the excitation frequency and its multiples (the amplitude is not small so the superharmonics can be due to nonlinearities); inside the instability region the response is non-stationary and changes is character depending on the modes activated, the spectrum is broadband.
Even if a specific analysis is not carried out yet, some conjectures can be made. The instability seems to lead to a chaotic region; the activation of several modes suggests that this could be high dimensional chaos.

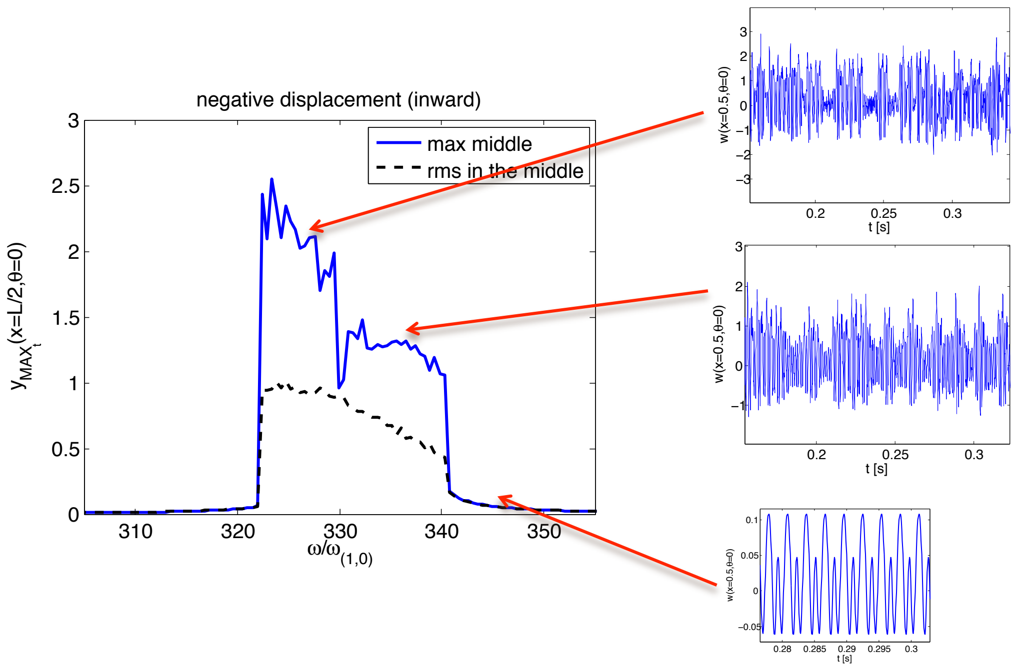

Figure 17. Time histories.

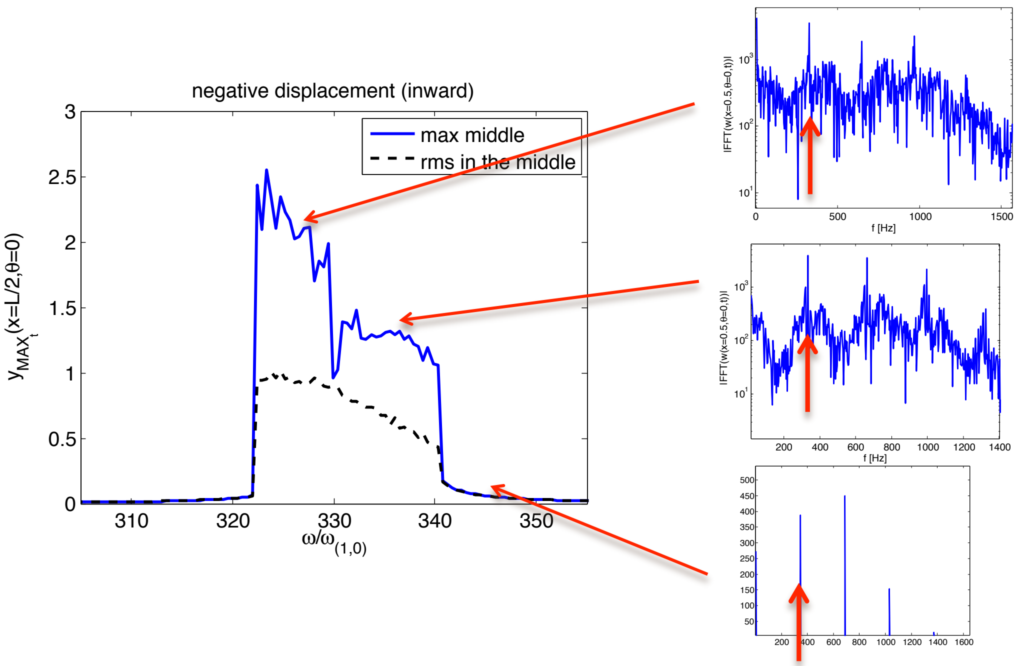

Figure 18. Spectra.

5 Conclusions

In this paper an experimental investigation on the nonlinear dynamics of circular cylindrical shells excited by a base excitation is presented. A nonlinear model of the shell considering also the shell shaker interaction is developed.

Experiments clearly show a strong nonlinear phenomenon appearing when the first axisymmetric mode is excited: the phenomenon leads to large amplitude of vibrations in a wide range of frequencies, it appears extremely dangerous as it can lead to the collapse of the shell; moreover, it appears suddenly both increasing and decreasing the excitation frequency and is extremely violent. By observing experimentally a strong transfer of energy from low to high frequency a conjecture can be made about the nonlinear interaction among axisymmetric (directly excited) and asymmetric modes. A saturation phenomenon regarding the vibration of the top disk is observed, this is associated with the violent shell vibration; the shell behaves like an energy sink, absorbing part of the disk energy.

The theoretical model shows satisfactory agreement with experiments and clarifies the energy transfer mechanism from low frequency axisymmetric modes and high frequency asymmetric modes, confirming the conjecture arising by the experimental data analysis.

It is now clear that, in order to safely predict the response of a thin walled shell carrying a mass on the top, i.e. the typical aerospace problem for launchers, a nonlinear shell model is needed, but it is not enough: a further modelling regarding the shell mass interaction and the interaction between shell and excitation source is needed.

References

[1] Leissa, A.W., 1993. Vibration of Shells, NASA SP-288. Washington, DC: Government Printing Office. Now available from The Acoustical Society of America.

[2] Babcock, C.D., 1983. Shell Stability. Journal of Applied Mechanics, 50, 935-940.

[3] Calladine, C.R., 1995. Understanding Imperfection-Sensitivity in the Buckling of Thin-Walled Shells. Thin-Walled Structures, 23, 215-235.

[4] Teng, J.G., 1996. Buckling of thin shells: Recent advances and trends. Applied Mechanics Reviews, 49(4), 263-274.

[5] Amabili, M., Païdoussis, M.P., 2003. Review of studies on geometrically nonlinear vibrations and dynamics of circular cylindrical shells and panels, with and without fluid-structure interaction. Applied Mechanics Reviews, 56, 349-381.

[6] Amabili, M., 2008. Nonlinear Vibrations and Stability of Shells and Plates, Cambridge University Press, Cambridge.

[7] Kubenko, V.D., Koval'chuk, P.S., 1998. Nonlinear problems of the vibration of thin shells (review). International Applied Mechanics. 34, 703- 728.
[8] Pellicano, F., 2007. Vibrations of circular cylindrical shells: theory and experiments. J. of Sound and Vibration, **303**, 154–170. doi:10.1016/j.jsv.2007.01.022.
[9] Mallon, N. J., Fey, R. H. B., Nijmeijer, H., 2010. Dynamic stability of a base-excited thin orthotropic cylindrical shell with top mass: Simulations and experiments. J. of Sound and Vibration, 329, 3149-3170.
[10] F. Pellicano, Dynamic instability of a circular cylindrical shell carrying a top mass under seismic excitation: experiments and theory, Int. J. of Solids and Structures, 48 (2011) 408–427.